Chemical deposition of PbS thin films under alternating magnetic field of 0, 25 and 50 Hz

BARIŞ ALTIOKKA[*], AYÇA KIYAK YILDIRIM[*]
Bilecik Şeyh Edebali University, Bilecik 11210, Turkey

Thin films of PbS were produced by chemical bath deposition method under alternating magnetic field. A coil was wrapped surrounds the bath container. Two terminal of coil were connected a power supply. The frequencies of the alternating magnetic field were varied of 0, 25 and 50 Hz. Besides, the magnitudes of the magnetic field were determined as to be 0, 3.25 and 6.5 mT. Structural analyses of the films were performed by an X-ray diffractometer. There were two texture coefficients at (111) and (002) planes, greater than 1, of the film obtained without the magnetic field. The magnetic field varied preferred orientation. On the other hand, the films obtained under the magnetic field showed preferred orientation at (111) plane. Crystallite sizes of the samples were calculated by using XRD results. Besides, magnetic field effected crystallite size. Crystallite size of the PbS films obtained without magnetic field was 62 nm and others were average 50 nm. The surface morphologies were investigated by using a scanning electron microscope (SEM). When surface was investigated with 30000 times magnified, pinholes and voids were not seen and sizes of the polymorphic crystal were varied between 200 nm and 1000 nm.

(Received February 25, 2019; accepted October 9, 2019)

Keywords: PbS, Lead sulfide, Chemical bath deposition, Thin films

---

1. Introduction

Narrow energy gap semiconductors are of great interest because of their unique properties and applications. Lead sulphide (PbS) which is one of these semiconductors has a relatively small band gap (0.41 eV at 300 K) and therefore can be used for fabrication of mid-infrared detectors ($3<\lambda<30$ μm) [1]. It has the optical absorption coefficient of $>10^5$ cm^{-1}. Both p- and n-type can be obtained by doping. PbS has been also recommended as an earth-abundant sustainable material for affordable photo voltaic [2].

There are a variety of methods, such as chemical vapor deposition (CVD), spray pyrolysis (SP) and thermal evaporation (TE) which have been traditionally used to prepare PbS thin films, but each technique has shown some limitations. These methods require high temperatures to enable the successful formation of thin films [3]. Among these methods, chemical bath deposition (CBD) is of special interest as it is a simple and highly efficient method [4–6]. It is also known as the solution growth. It allows potent and adjustable control of the size and surface density of nanoparticles. Therefore, it can be used for the preparation of high-quality nanocrystalline PbS films by controlling the deposition parameters such as bath temperature, stirring period, solution pH, reaction time and added impurities [7].

The deposition mechanism for PbS precipitation is as follows [8].

$$Pb(NO_3)_2 + 2NaOH \rightarrow Pb(OH)_2 + 2NaNO_3 \quad (1)$$

$$Pb(OH)_2 + 2NaOH \rightarrow Na_2\left[Pb(OH)_4\right] \quad (2)$$

$$\left[Pb(OH)_4\right]^{2-} \rightarrow Pb^{2+} + 4OH^- \quad (3)$$

$$CS(NH_2)_2 + OH^- \rightarrow CH_2N_2 + H_2O + HS^- \quad (4)$$

$$HS^- + OH^- \rightarrow H_2O + S^{2-} \quad (5)$$

When the ionic product of Pb^{2+} and S^{2-} ions exceed the solubility product of PbS (1.1×10^{-29}), the insoluble crystals of PbS precipitate [8].

$$Pb^{2+} + S^{2-} \rightarrow PbS \quad (6)$$

There are plenty of studies on the investigation of PbS obtained by CBD. Nearly in all these studies, surface images have been investigated. Only one of them showed relatively low magnified surface images[9]. It revealed that pinholes and voids could not be seen on relatively high magnified surface images but they could be seen on relatively low magnified surface images. Besides, it also showed that decreasing reaction rate prevented forming of pinholes and voids.

In this study, the reaction rate was tried to be reduced by the magnetic field. It was understood from the XRD patterns that magnetic field changed the preferred orientation of PbS crystals.

2. Experimental procedure

Aqueous solutions of 0.009M lead nitrate (Pb(NO3)2), 0.15M sodium hydroxide (NaOH) and 0.051M thiourea (CS(NH2)2) was used to deposit PbS thin films chemically. The deposition bath container and glass substrates were washed with acetone and thereafter they were washed with deionized water. The depositions were completed in 40 minutes and bath temperatures were kept at 25±1°C during the depositions.

The depositions were carried out under five conditions and they were named p1-p5 according to the magnitude and frequency of the magnetic field as given in Table 1. For applying the magnetic field, the mechanism given in Fig. 1 was used. The final solutions were stirred 600rpm for magnetic field effected ions in the solutions.

Table 1. Tabulated depositions conditions

Exp. No	**$Pb(NO_3)_2$**	**NaOH**	**$CS(NH_2)_2$**	**Frequency**	**Magnetic field**	**Film Thickness**
	(M)	**(M)**	**(M)**			
P1	0.009	0.15	0.051	0	0	780nm
P2	0.009	0.15	0.051	25Hz	3.25mT	513nm
P3	0.009	0.15	0.051	50Hz	3.25mT	508nm
P4	0.009	0.15	0.051	25Hz	6.50mT	497nm
P5	0.009	0.15	0.051	50Hz	6.50mT	491nm

Table 2. Calculated texture coefficients according to the various plane

Experiments	**P1**	**P2**	**P3**	**P4**	**P5**
T.C.(111)	1.089	1.329	1.284	1.467	1.322
T.C.(002)	1.127	0.765	0.759	0.587	0.758
T.C.(022)	0.785	0.908	0.957	0.946	0.914

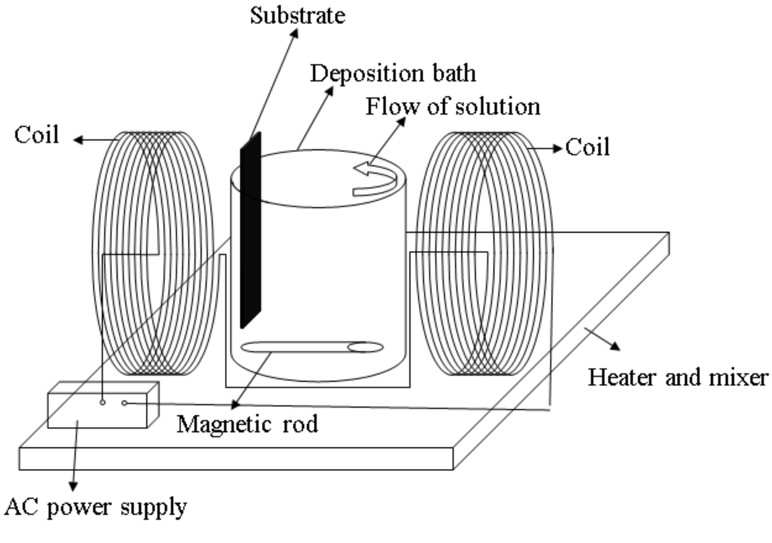

Fig. 1 Schematic representations of deposition mechanism

The film thicknesses were calculated by using the gravimetric method. Unilab teslameter was used to measure the magnitude of magnetic field. A PANalytical Empyrean XRD (X-ray diffractometer) was employed to analyze structural properties of the PbS thin films. A Zeiss SUPRA 40VP SEM (scanning electron microscope) was used for analyzing the surface morphology of the PbS thin films.

3. Result and discussion

3.1. Structural studies of PbS thin films

Well known gravimetric method was used for calculating thicknesses of the films ($t = \frac{m}{\rho A}$) where t is the film thickness, ρ is the density of PbS, m is the mass of the present film and A is the surface areas of deposited samples [10]. Film thicknesses were calculated by using the gravimetric method and the results are given in Table 1.

While the thicknesses of the films obtained under magnetic field were being varied between 491nm and 513nm, the thickness of the film obtained without the magnetic field was 780nm. This result showed that magnetic field reduced the reaction rate. It was concluded that magnetic force might scattered ions in the final solution and thus, reaction rates were reduced.

X-ray diffractometer patterns for the produced PbS films are given in Fig. 2 and they revealed that all films were formed in cubic galena structure with same as in the literature [11] (ASTM card no 98-060-0243). The texture coefficients, given in Eq. 7 [12], of the films were employed for the determination of the preferred orientation.

$$TC = \frac{I_{(hkl)}/I_{0(hkl)}}{\frac{1}{N}\sum_{N}(\frac{I_{(hkl)}}{I_{0(hkl)}})} \tag{7}$$

where I(hkl)was the measured relative intensity of a plane (hkl), I0(hkl) was the standard intensity of the plane (hkl) given in ASTM card. The calculated texture coefficients are given in Table 2.

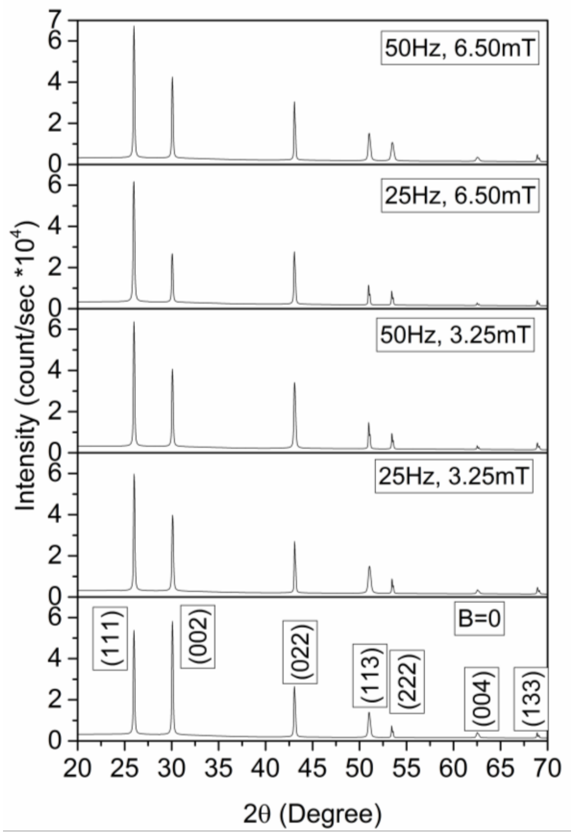

Fig. 2. X-ray diffractograms of PbS thin films deposited under various magnetic field

Table 3. Structural values of the PbS thin films

Exper.	Crystallite Size (nm)	Lattice parameter a(corrected) (Å)	Micro strain *10^{-3}	Average Stress (10^{9}N/m^2)	Dislocation Density (lines/m^2) *10^{14}
P1	62	5.937	0.17	0.0211	2.601
P2	43	5.944	1.35	0.1692	5.410
P3	53	5.947	1.19	0.1492	3.560
P4	51	5.949	2.19	0.2745	3.845
P5	54	5.947	1.19	0.1492	3.429

According to the texture coefficients, although the films produced under the magnetic field showed preferred orientation of (111) plane, the peak intensity of (002) plane of the film obtained without the magnetic field was higher than that of the (111) plane. This result was an expected result in compliance with the literature. In a previous study [13], when reaction rate was reduced, the preferred orientation shifted from the (002) plane to the (111) plane as in this study. This result might be the other evidence that reaction rates were reduced by the magnetic field.

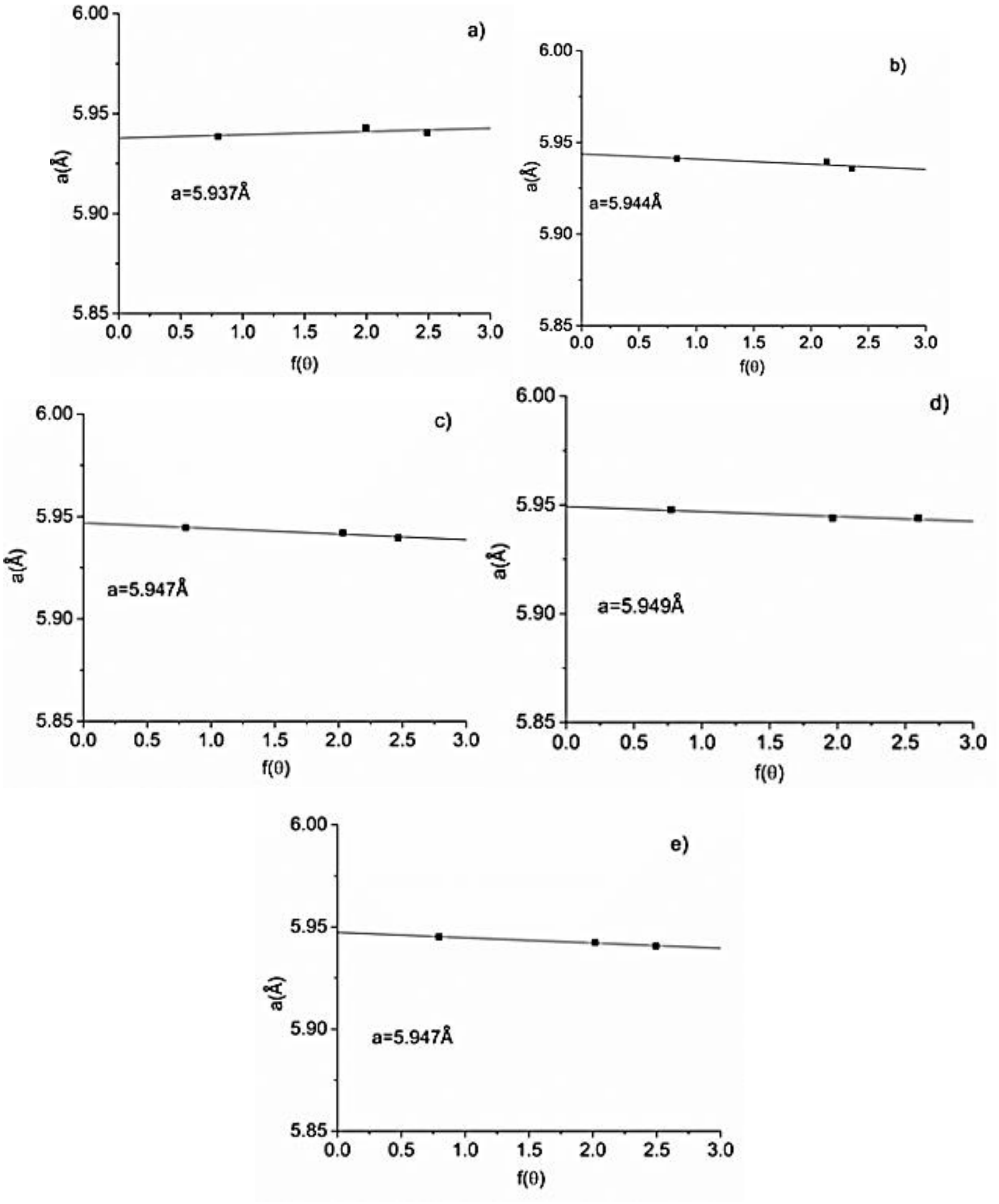

Fig. 3. Nelson–Riley plots of PbS thin film obtained under a) 0mA, 0mT b) 25Hz, 3.25mT c) 50Hz, 3.25mT, d) 25Hz, 6.50mT and e)50Hz, 6.50mT magnetic field

The average crystallite sizes of samples were estimated Debye Scherrer equation given in Eq. 8.

$$cs = \frac{0.9*180*\lambda}{3.14*\beta*\cos\theta_C} nm \qquad (8)$$

where λ was the wavelength of X-ray radiation (1.54056 Å), β was the full width half maximum, $2\theta_C$ was the Bragg angle and were obtained from the XRD data, β and 2θC were calculated by fitting the XRD peak profile [14]. The estimated crystallite sizes of the films are given in Table 3.

The lattice constant of the cubic rock salt structure was given as follows [15]

$$a = d\sqrt{(h^2 + k^2 + l^2)} \qquad (9)$$

where h, k and l were the Miller indices and d was the interplanar distance.

The micro strain and average stress were calculated by using Eq. 10 and 11 respectively which are given in Table 3.

$$\varepsilon = (a_0 - a)/a_0 \tag{10}$$

$$S = \varepsilon Y/(2\sigma \tag{11}$$

where a0 and a were lattice parameter of the bulk sample and the corrected value of lattice parameter of thin film samples respectively. The σ and Y were the Poisson's ratio and Young's modulus of the bulk crystal respectively. For PbS the value of Y was 70.2 GPa and σ was 0.28. The corrected values were estimated from the Nelson–Riley plots given in Fig. 3. The lattice parameters calculated from the peak positions of individual reflections were plotted against $F(\theta) = (cos^2\theta/2) * (\frac{1}{sin^2\theta} + \frac{1}{\theta})$ and the intercept of the linear plot at $(cos^2\theta/2) * (\frac{1}{sin^2\theta} + \frac{1}{\theta}) = 0$ gave the corrected lattice constant [11]. Deviation of the calculated lattice parameter (a) from the strain face bulk sample (a0 = 5.936 nm) indicated that the obtained films were under strain [16]. The micro strain and stress of the film obtained without magnetic field were lower than that of the other films. It was concluded that this might result due to relatively high crystallite size.

Dislocation density could be derived from the crystallite size as given in Eq. 12 [17]

$$\delta = \frac{1}{(cs)^2} \tag{12}$$

The calculated dislocation density of the film obtained without magnetic field was nearly half of that of the other films due to the fact that it had relatively high crystallite size.

3.2. Surfaces of PbS thin films

The 30000 times magnified surface images are given in Fig. 4. These surfaces were seen with the typical morphology of PbS films. The sizes of the polymorphic particles varied between 200 nm and 1000 nm. It was noteworthy that there were no pinholes and voids on these surfaces. These surfaces are like as in the literature [18].

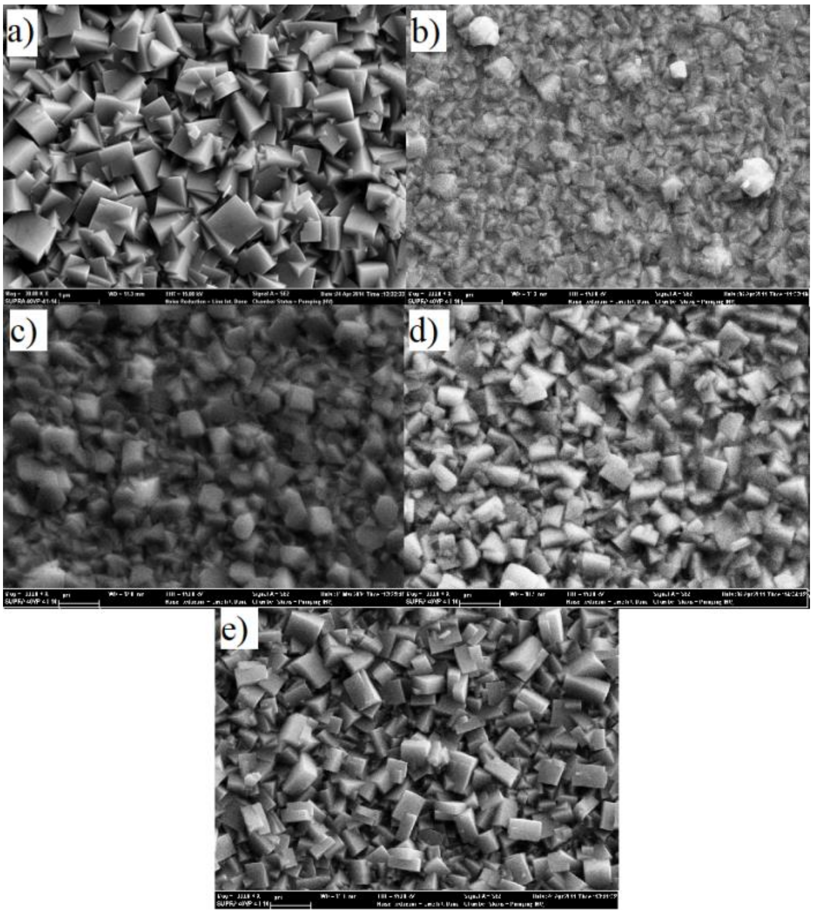

Fig. 4. 30000 times magnified SEM photographs of the PbS films obtained under a) 0mA, 0mT b) 25Hz, 3.25mT c) 50Hz, 3.25mT, d) 25Hz, 6.50mT and e)50Hz, 6.50mT magnetic field

4. Conclusions

In this work, PbS thin films were produced by chemical bath deposition. In some experiments, depositions were carried out under magnetic field. It was inferred from the film thicknesses and texture coefficients that reaction rate was reduced by the magnetic field. It might be derived from that magnetic field might cause scattering ions in the final solutions. Pinholes and voids there should not be in the p-n or junctions because of the fact that they might cause short circuits.

This study showed that when reaction rate was reduced, pinhole and void formations were prevented by the magnetic field and compact and smooth surfaces might be obtained by applying the magnetic field.

References

[1] A. P. Gaiduk, P. I. Gaiduk, A. Nylandsted, Thin Solid Films **516**, 3791 (2008).
[2] N. B. Kotadiya, A. J. Kothari, D. Tiwari, T. K. Chaudhuri, Appl. Phys. A **108**, 819 (2012).
[3] A. S. Obaid, M. A. Mahdi, Z. Hassan, M. Bououdina, Int. J. Hydrogen Energy **38**, 807 (2012).
[4] E. Güneri, F. Göde, B. Boyarbay, C. Gümüş, Mater. Res. Bull. **47**, 3738 (2012).
[5] F. Göde, F. Yavuz, I. A. Kariperb, Acta Phys. Pol. A **128**, 215 (2015).
[6] F. Göde, Optik **197**, 163217 (2019).
[7] T. Tohidi, K. Jamshidi-Ghaleh, Appl. Phys. A Mater. Sci. Process. **118**, 1247 (2014).
[8] E. Pentia, L. Pintilie, T. Botila, I. Pintilie, A. Chaparro, C. Maffiotte, Thin Solid Films **434**, 162 (2003).
[9] B. Altıokka, Arab. J. Sci. Eng. **40**, 2085 (2015).
[10] F. Göde, S. Ünlü, Open Chem. **1**, (2018).
[11] F. Göde, S. Ünlü, Mater. Sci. Semicond. Process. **90**, 92 (2019).
[12] H. Soetedjo, B. Siswanto, I. Aziz, S. Sudjatmoko, J. Babarsari, J. Non-Oxide Glasses **9**, 55 (2017).
[13] B. Altıokka, M. C. Baykul, M. R. Altıokka, J. Cryst. Growth **384**, 50 (2013).
[14] R. Bhowmik, M. N. Murty, E. S. Srinadhu, PMC Phys. B **1**, 20 (2008).
[15] A. Hussain, A. Begum, A. Rahman, Indian J. Phys. **86**, 697 (2012).
[16] S. Rajathi, K. Kirubavathi, K. Selvaraju, Arab. J. Chem. **10**, 1167 (2017).
[17] A. N. Fouda, M. Marzook, H. M. Abd El-Khalek, S. Ahmed, E. A. Eid, A. B. El Basaty, Silicon **9**, 809 (2017).
[18] L. Raniero, C. L. Ferreira, L. R. Cruz, A. L. Pinto, R. M. P. Alves, Phys. B Condens. Matter **405**, 1283 (2010).

---

[*] Corresponding author: baltiokka@gmail.com
ayca.kiyak@bilecik.edu.tr